Fourth International Symposium on Marine Propulsors
smp'15, Austin, Texas, USA, June 2015

Vortex Structure Characterization of Tip-Loaded Propellers

Michael Brown[1,2], Seth Schroeder[1], Elias Balaras[2]

[1] Naval Surface Warfare Center, Carderock Division, Bethesda, MD 20817, USA
[2] Department of Mechanical and Aerospace Engineering, George Washington University, Washington DC 20052, USA

ABSTRACT

Tip-loaded propellers (TLPs) have been shown to increase efficiency by shifting the loading distribution toward the tip while using a pressure-side winglet to prevent associated losses. The winglet prevents the formation of a single strong tip vortex, and instead two distinct weaker vortices are shed. The interaction between the two tip vortices with each other and the downstream wake is unknown and could significantly affect cavitation performance. Through computations we will investigate the impact of the tip vortex/wake interaction on the TLP propeller performance characteristics, with a focus on tip vortex evolution. RANS calculations as well as high-fidelity Large-Eddy simulations are qualitatively and quantitatively compared to recent cavitation tunnel experiments, and further conclusions are drawn from the highly-resolved three dimensional flow field.

Keywords

Propellers, Efficiency, Tip Vortex, Large Eddy Simulation, Immersed Boundary Method.

1 INTRODUCTION

Improving propulsive efficiency is a perpetual goal for naval architects and engineers. The tip-loaded propeller (TLP, Brown et al., 2014) and the Contracted Loaded Tip (CLT ®) propeller (Adalid and Gennaro, 2011) have been demonstrated to improve propeller efficiency by shifting the spanwise loading distribution towards the tip of the propeller while using a pressure-side winglet to prevent associated losses. In principle, this is similar to how airplane winglets improve lift-to-drag ratio.

For conventional propellers increasing the circulation in the outer portion of the span tends to increase the strength of the tip vortex and therefore reduce the cavitation inception speed. For propellers with strict cavitation inception requirements, such as those of naval ships or special applications where radiated noise is a priority, (Michael et al., 2000) the strength and characteristics of the tip vortex must be carefully controlled. The pressure side winglet of the TLP will improve the tip vortex cavitation performance by preventing the formation of a very low pressure in the core of a single, strong tip vortex. However, the behavior of the vorticity in the wake of a TLP is not fully understood, and as such its strength and characteristics will continue to be a concern during future TLP design cycles.

During recent experiments on a US Navy designed TLP, interesting tip vortex structures were witnessed in the cavitation tunnel. Two cavitating, co-rotating tip vortices were generated by each propeller blade. One vortex was shed from the blade/endplate junction, while another was shed from the outermost edge of the endplate. The two cavitating vortices remained separate for an axial distance of approximately ½ of the diameter, at which point they merged into a single cavitating vortex.

Previous work in the area of propulsor tip vortex characterization has seen fairly similar co-rotating structures at the tips of ducted propulsors (Hsiao and Chahine, 2004). In that case, a dominant "leakage" vortex was shed from approximately the midchord of the blade tip, while a weaker vortex was shed from the trailing edge of tip. The leakage vortex and the trailing edge vortex remained distinct for less than one chord length downstream before they merged into one cavitating vortex. For these types of propulsors, successful predictions of the minimum pressures in the tip vortices were made using a hybrid RANS/DNS method and an overset technique. One of the conclusions of the study was that minimum pressures did occur in the region of the merging of the two vortices. In that study, as well as the recent TLP analyses, the RANS methods were too diffusive to capture the vortices accurately a sufficient distance away from the blade in order to make accurate predictions of cavitation inception. To overcome these limitations, in the present work we will use highly resolved large-eddy simulations (LES) to capture the dynamics of the tip vortices for relatively large distances in the wake. We have successfully used this approach for the analysis of a nominal submarine propeller with very good results (Schroeder et al. 2014)

2 DESCRIPTION OF THE EXPERIMENTS

2.1 Model scale hardware

A model of the NSWCCD TLP was constructed of bronze at 1/26th scale. The diameter of the model-scale propeller

was 250mm. The model was constructed by the model manufacturing facility at the Canal de Experiencias Hidrodinámicas de El Pardo (CEHIPAR).

The NSWCCD tip loaded propeller (TLP) model as fabricated by CEHIPAR using bronze is shown in Figure 1. It was designed for a spanwise circulation distribution with a maximum at 0.80R. The TLP includes a blended, pressure side winglet designed using NSWCCD blade shaping methods modified for use on TLPs. The blade sections include a NACA 66 thickness distribution and a custom chordwise loading distribution with more trailing edge loading than the more traditional NACA a=0.8.

The TLP was designed for a thrust loading coefficient (C_T) and advance coefficient (J_A) of 1.27 and 0.923, respectively. A more detailed description of this propeller design can be found in Brown, et al. (2014).

Figure 1: NSWCCD tip loaded propeller (TLP) model scale hardware.

2.2 Open Water Experiment

The open water tests were conducted in the calm water towing tank at CEHIPAR. The rotational speed of the models was set at 15 revolutions per second (RPS), and the speed of the carriage was varied in order to obtain thrust and torque values over a range of advance coefficients. The Reynolds number for the open water experiments at the design advance coefficient was approximately 4.32×10^5, as defined by:

$$Re = \frac{c_{0.7R}\sqrt{(V_A^2 + (0.7\pi nD)^2}}{\upsilon}$$

Where $c_{0.7R}$ is chord length at r/R=0.7, V_A is the speed of advance, n is the rotational velocity, ν is the kinematic viscosity and D is the propeller diameter.

2.3 Cavitation Tunnel Experiment

Cavitation inception and pressure pulse measurements were conducted in the cavitation tunnel at CEHIPAR. The nominal rotational speed of the models was again 15 RPS and resulted in similar Reynolds numbers as the open water experiments. Tunnel corrections for measured thrust and torque were not performed in this case as the model disk area to tunnel area ratio was 0.061. A thrust identity method was used to set conditions in the tunnel.

In addition to the inception and pressure pulse measurements, high-speed video was taken of the TLP in the cavitation tunnel at multiple operating conditions. These videos were post-processed to produce images of the tip vortex cavitation that will be used to make both qualitative and quantitative comparisons to the LES results. Of particular interest is the propeller operating in at the design advance coefficient, but with a lower pressure than the design operating point. The reduced pressure serves to accentuate the tip vortex cavitation, enhancing its use for flow visualization. This is shown in Figure 2.

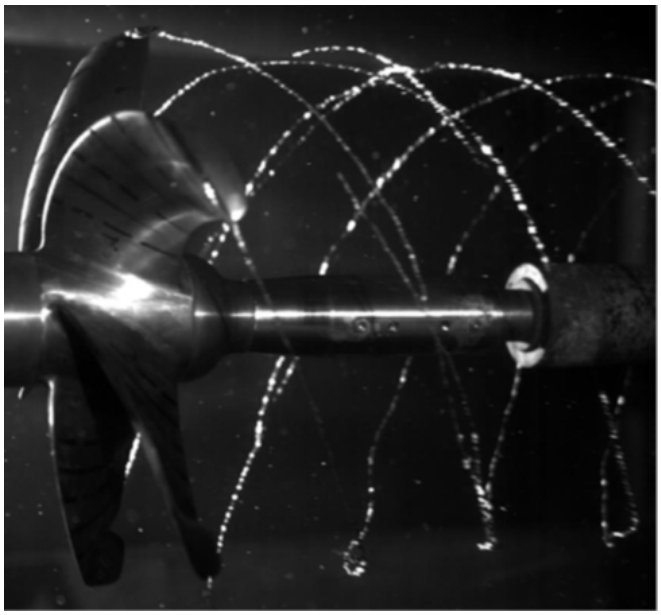

Figure 2: Image of the TLP in the CEHIPAR cavitation tunnel.

3 DESCRIPTION OF THE VISCOUS SOLVERS

3.1 NavyFOAM RANS Solver

NavyFOAM is an unstructured, finite-volume based flow solver with RANS and LES capabilities. The version used for this project was a single-phase RANS solver in a rotating reference frame. One blade passage was gridded and periodic boundary conditions were employed to include the effects of the other four blades of the propeller. The domain was discretized with a block-structured, body-fitted mesh using ANSYS ICEMCFD software. A semi-circular trailing edge geometry of 0.2mm radius was modeled in the grid. Wall functions were used to simulate the boundary layer, and a y+ at the wall of 30 was taken as a target. For this study, the H. R. Wilcox k-Omega turbulence model was used. A more complete description of the NavyFOAM RANS solver and validation for rotating propulsors can be

found in Kim et al. (2010). The CEHIPAR cavitation tunnel hub geometry was included in the grid, and consists of a bullet-shaped nosecone upstream and a faired taper down to a smaller diameter driveshaft downstream.

During the NavyFOAM analysis of the TLP, a grid sensitivity study was performed at multiple advance coefficients. Through this study, model-scale grids of approximately 2.0 million cells and full-scale grids of approximately 2.6 million cells were selected. An example of the blade surface discretization is shown in Figure 3 for the TLP.

These computations were performed on NSWCCD's internal cluster, and used between 24-32 processor cores.

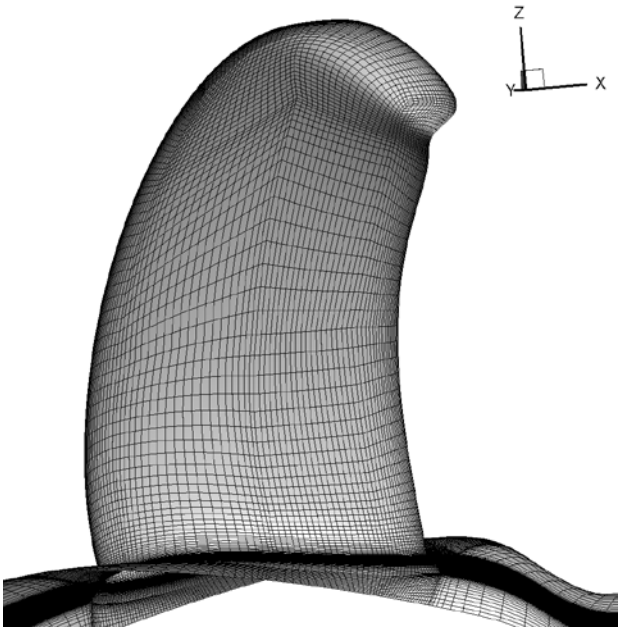

Figure 3: Blade surface mesh for TLP NavyFOAM full-scale Reynolds number analyses.

3.2 Large Eddy Solver with Immersed Boundaries

To capture the dynamics of the tip vortices and their interaction in the wake of the propeller an eddy-resolving methodology, such as LES, needs to be adopted. Furthermore, because the area of interest extends relatively far downstream from the propeller, a solver with non-dissipative discretizations and optimal conservation properties is desired. In the present work, the spatially filtered versions of the Navier-Stokes equations for incompressible flow are solved on a structured grid in cylindrical coordinates. The equations are advanced in time with a semi-implicit fractional step method, where the advective and diffusive terms in the azimuthal direction are treated implicitly with a Crank-Nicolson scheme, while all the other terms are treated explicitly with a third-order Runge-Kutta method. All spatial derivatives are approximated with second-order central differences on a staggered grid. Boundary conditions on the rotating propeller blades, which are not aligned with the grid lines, are imposed using an immersed boundary formulation. The overall accuracy of the method is second order in both space and time (see Balaras 2004 for details). This methodology has been applied previously to marine propulsors (see Schroeder, 2014) as well as complex turbomachinery applications (see Posa et al., 2011, 2015) with results in excellent agreement to the corresponding experiments. In the former study, grid resolution tests established a required grid resolution for a propeller at a model scale Reynolds number. That grid resolution requirement was exceeded for this study. The grid spacing is shown in Figure 4. The grid was numerically generated using a piece-wise continuous spacing, as shown in the lower portion of Figure 4. This creates a continuous point distribution, shown in the upper portion of the figure.

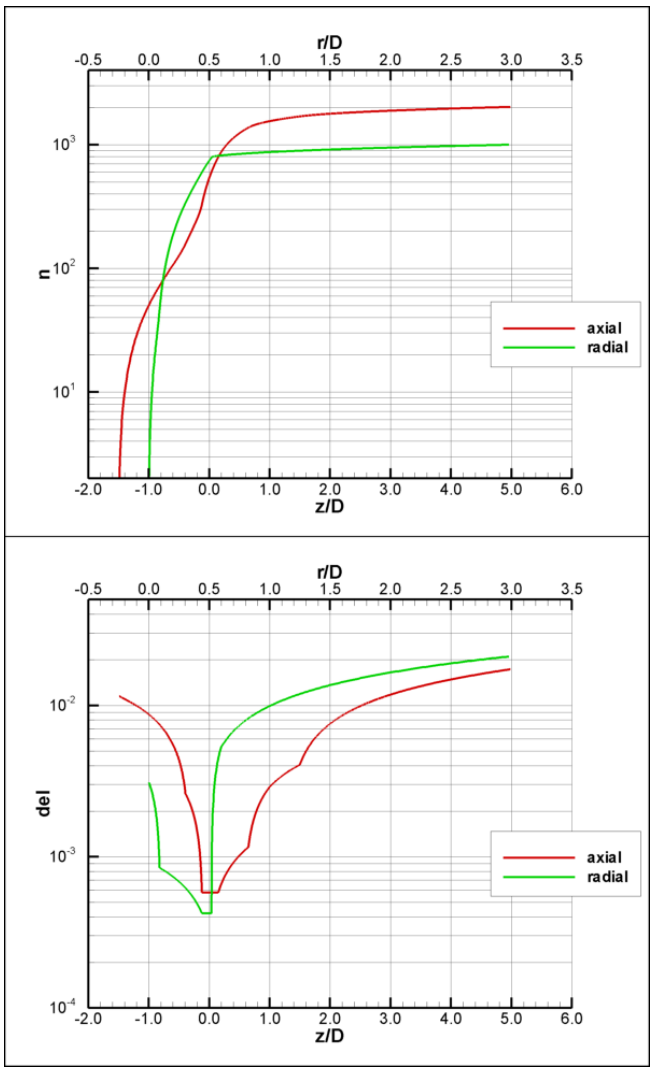

Figure 4: Index number vs. axial and radial coordinate (upper), and grid spacing vs. axial and radial coordinate (lower).

The subgrid scale model used for this study is the Wall-Adapting Local Eddy-viscosity (WALE) model, as proposed by Nicoud & Ducros (1999). The WALE model was recently tested by Weickert et al. (2010), and shown to accurately predict transition from laminar to turbulent flow.

All LES computations were performed on the US Navy DSRC CRAY supercomputer *Shepard*, using between 256 and 1,000 processor cores.

4 RESULTS

4.1 Integrated forces

Measuring the open water thrust and torque was necessary to establish the conditions for the cavitation experiments, as well as to check the accuracy of the RANS and LES computations. Figure 5 shows comparisons of the thrust, torque and efficiency of the TLP, from both the experiments and computations.

The solid lines represent the experimental data while symbols indicate the results of the computations, with filled symbols showing the NavyFOAM results and hollow symbols showing the LES results. The vertical line represents the design advance coefficient. The nomenclature for thrust, torque and efficiency follows the standard ITTC definition and are provided here:

$$K_T = \frac{T}{\rho n^2 D^4}$$

$$K_Q = \frac{Q}{\rho n^2 D^5}$$

$$ETAo = \frac{J_A * K_T}{2\pi * K_Q}$$

Both the RANS and the LES calculations show excellent agreement with the experiment. The thrust and torque from the computations are within 2% of the experimental data for all of the computed advance ratios.

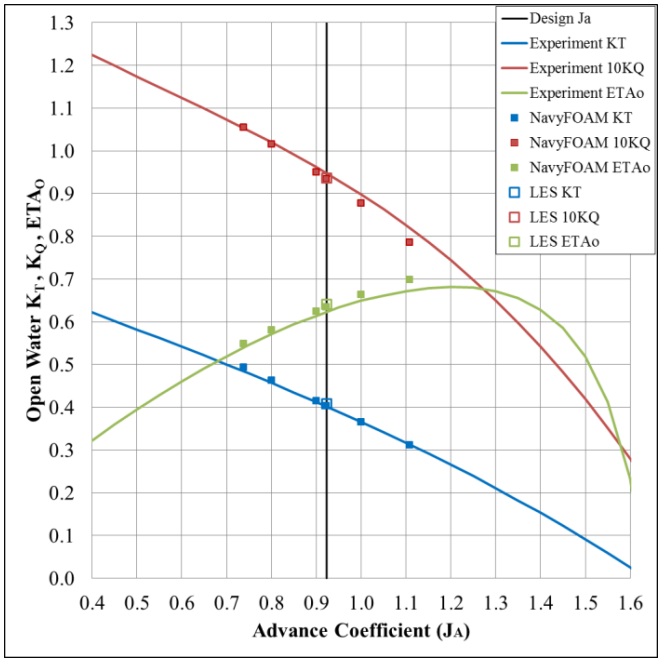

Figure 5: Open water thrust, torque and efficiency of TLP from experiment, RANS and LES.

4.2 Tip vortex evolution

The RANS computations did capture the dual vortex structure generated by the TLP, demonstrated in Figure 6. However, as shown in Figure 7, the discrete nature of vortical structures was lost before Z/D=0.2, and the tip vortex was entirely dissipated after Z/D=0.4.

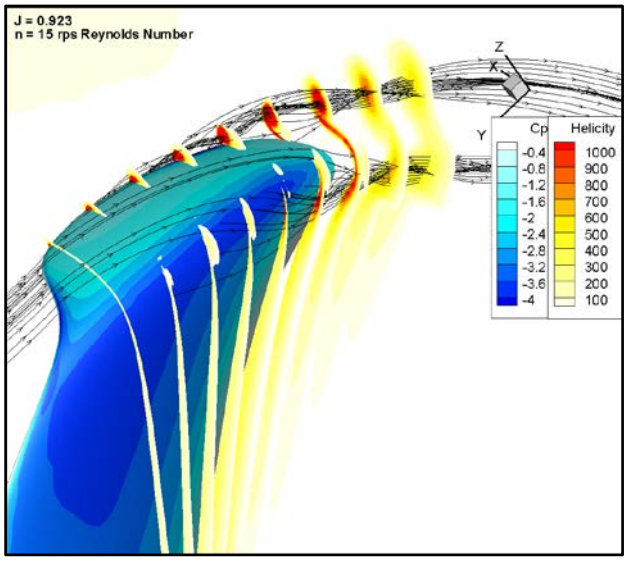

Figure 6: Contours of helicity, pressure and streamtraces from RANS solution.

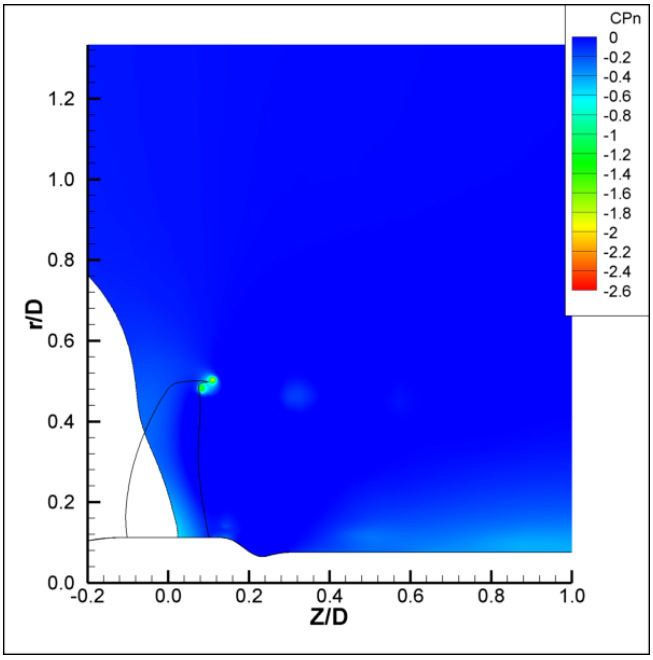

Figure 7: R-Z slice of RANS solution, demonstrating early vortex dissipation.

In the case of LES, the tip vortices were visualized in three dimensions by plotting an isosurface of pressure. This is shown in Figure 8, where the isosurface is plotted at a CP_n= 1.2. The color of the isosurface represents the axial coordinate. For plotting purposes, the data is only shown between axial values of 0.05 and 0.6. CP_n is defined below:

$$CP_n = \frac{P}{0.5\rho n^2 D^2}$$

The results are also visualized in two dimensions by plotting contours of pressure on R-Z and R-theta planes, shown in Figure 9 and Figure 10, respectively. The dynamics are similar to the cavitation tunnel experiment (Figure 2), where dual, co-rotating tip vortices are shed from the blade/endplate junction as well the edge of the endplate. Furthermore, in the LES there is a region near the trailing edge where the blade/endplate junction vortex is less coherent. This is also seen in the experiments, in that the vortex cavitation is more intermittent near the blade (Figures 2, 11 & 12).

For more quantitative analysis of the tip vortex evolution, a photogrammetric technique was used to process the images from the cavitation tunnel experiment. A helix was constructed using a definition similar to those of early potential flow propeller tools. The helix geometry is defined by a pitch angle, a final contraction ratio and an initial contraction angle. The contraction angle decays as the contraction ratio approaches the final value. A starting point is taken to be the mid-chord of the propeller tip, and the helix is propagated downstream via a shooting method. The equations describing this process are presented below.

$$\frac{dx}{d\theta} = r_{tip} * \tan(\beta)$$

$$\frac{dr}{dx} = -\tan(\phi_C) * \frac{\frac{r}{r_{tip}} - R_C}{1 - R_C}$$

$$\theta_{i+1} = \theta_i + d\theta$$

$$x_{i+1} = x_i + \frac{dx}{d\theta} * d\theta$$

$$r_{i+1} = r_i + \frac{dr}{dx} * \frac{dx}{d\theta} * d\theta$$

Where θ is the azimuthal coordinate, β is the helical pitch angle, ϕ_C is the contraction angle, and R_C is the final contraction ratio.

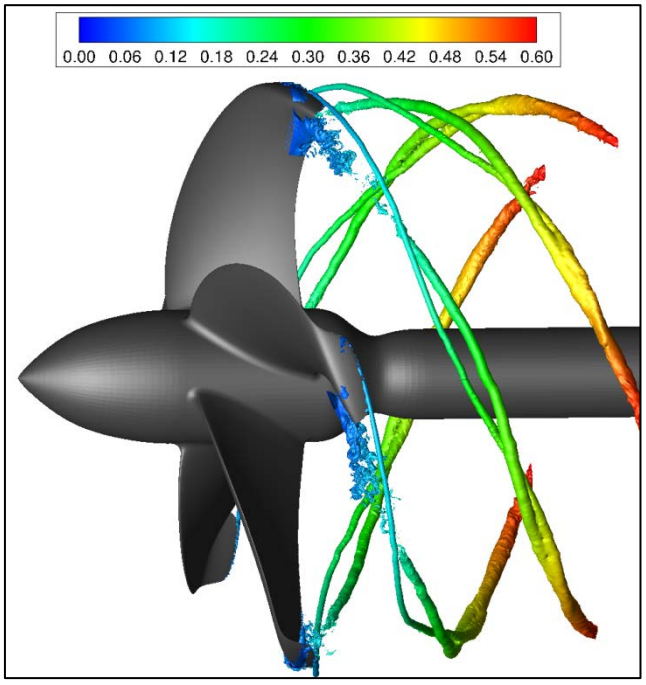

Figure 8: LES tip vortex tracking, shown by an isosurface of CP_n = -1.2, contours represent axial coordinate, Z/D.

The helical geometries generated by this method were then overlaid onto stills from the high-speed video taken during the cavitation experiment. The three parameters (β, ϕ_C, and R_C) were varied iteratively until values were found that provided a good match with the images from the experiments. Examples are shown in Figure 11 and Figure 12. The end results are quantitative values describing the evolution of the tip vortices that can be compared with

those of the LES solution. These values are presented in Table 1.

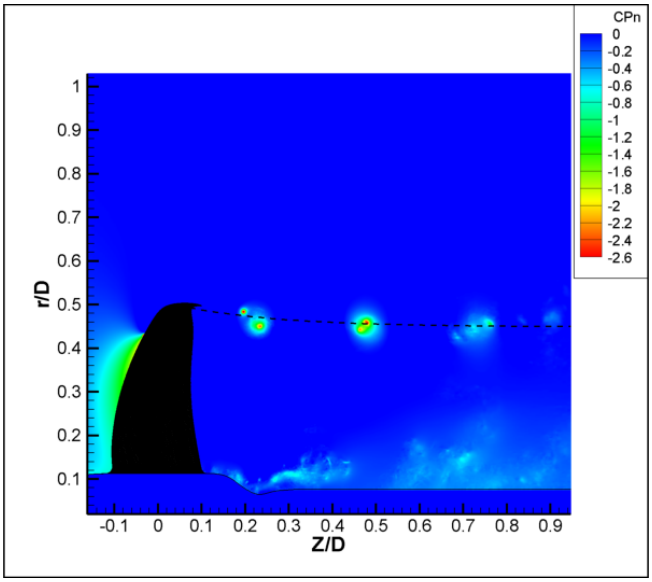

Figure 9: R-Z slice of LES data with contour of pressure, demonstrating tip vortex tracking.

Table 1: Tip vortex parameters of TLP at design conditions.

Parameter	Exp.	LES
Helical pitch (β)	21.5 degrees	22 degrees
Final contraction ratio (R_C)	0.9	0.9
Initial contraction angle (ϕ_C)	12 degrees	12 degrees

The LES tip vortex evolution matches the results of photogrammetric analysis of the cavitation tunnel images nearly identically, with the only difference being a half-degree of pitch. That being said, the margin of error on the photogrammetric analysis is not entirely known.

The results of the LES calculation show the merge location of the two tip vortices to be at approximately Z/D=0.48, as shown in Figure 8 and the bottom portion of Figure 10. This is also confirmed by the photogrammetric analysis of the cavitation tunnel images, which show the merge to take place to be in nearly the same location. The vortex merging is a highly unsteady process, so only approximate locations can be found from both the experiment and the LES without further statistical analysis.

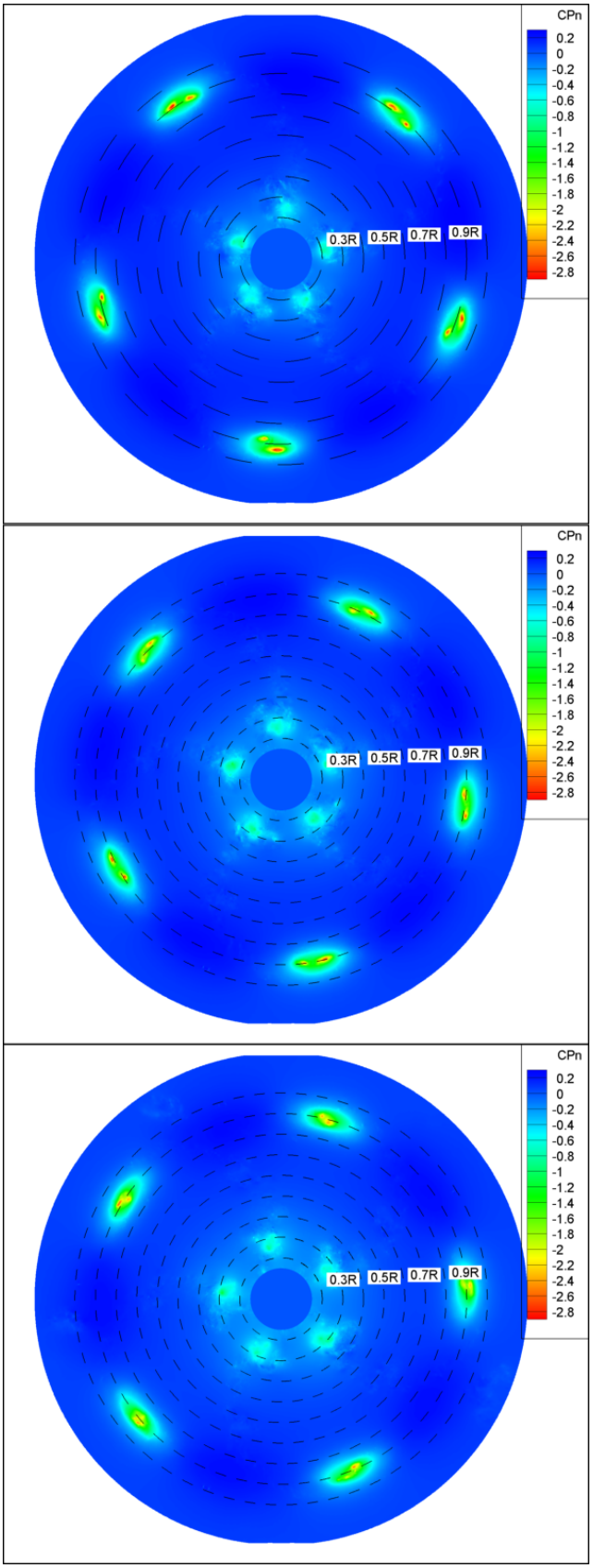

Figure 10: R-theta slices at three locations (Z/D = 0.40, 0.45 and 0.49) demonstrating vortices merging.

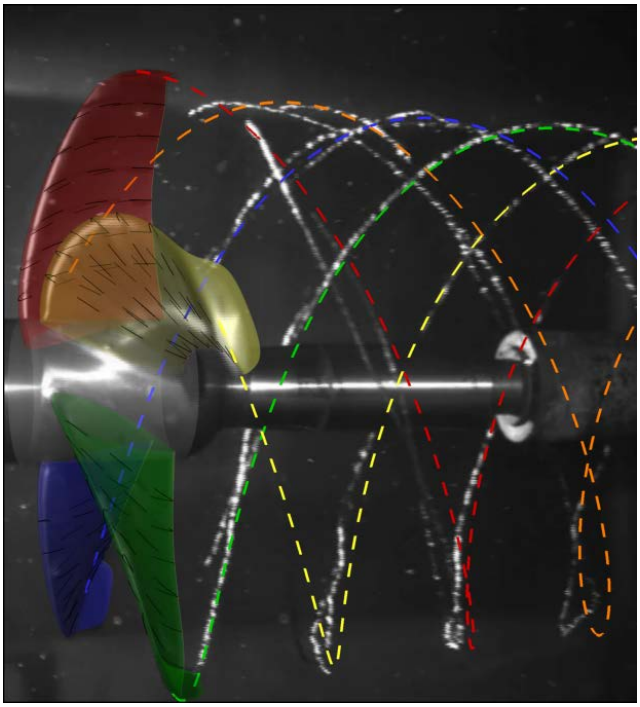

Figure 11: Example of tip vortex parameterization through photogrammetry (suction side view).

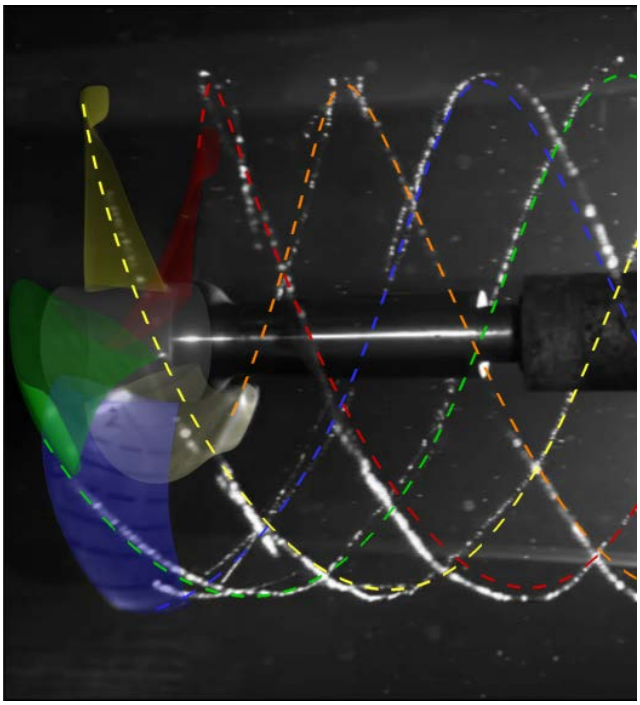

Figure 12: Example of tip vortex parameterization through photogrammetry (pressure side view).

5 CONCLUSIONS AND FUTURE WORK

The tip vortex of a novel propeller design was successfully studied through multiple computational methods.

While RANS analyses captured the formation of two tip vortices, they were not able to compute the evolution of the tip vortices or provide any insight into the vortex merging process. A LES coupled with an immersed boundary formulation accurately computed the evolution of the tip vortex, as verified with cavitation tunnel experiments.

Overall it appears that the separation of the two vortices has the effect of delaying the cavitation inception. It is expected that the separation between the two vortices will depend on a number of factors, some of those being the span of the endplate and the loading distribution of the endplate. In the case of the TLP design studied here, two vortices of nearly equal strength were developed entirely by accident. Future work includes confirming that the separation between the vortices delays the cavitation inception, and relating the design quantities of the tip to the generation and maintenance of separate tip vortices.

ACKNOWLEDGMENTS

Support for this research was provided by the Naval Surface Warfare Center, Carderock Division and the U.S. Office of Naval Research. The model construction and testing performed by CEHIPAR was funded through ONR NICOP Grant N62909-12-1-7087 managed jointly by Dr. Ki-Han Kim (ONR) and Drs. Richard Vogelsong and Woei-Min Lin at ONR Global. Funding for NSWCCD was provided by ONR Code 331, under the administration of Dr. Ki-Han Kim as well as from the Naval Surface Warfare Center, Carderock Division through an internal 219 project, monitored by Dr. Jack Price.

REFERENCES

Adalid, J. G., and Gennaro, G., (2011), "Latest experiences with Contracted and Loaded Tip (CLT) propellers." Sustainable Maritime Transportation and Exploitation of Sea Resources, 1st ed., Vol. 1, Taylor & Francis Group, London, pp. 47-53.

Balaras, E. (2004), "Modeling complex boundaries using an external force field on fixed Cartesian grids in large-eddy simulations." Computers and Fluids, 33, 375-404.

Beratlis, N. (2008), Direct Numerical Simulations of Transitional Pulsatile Flows in Stenotic Vessels, PH.D dissertation, University of Maryland.

Brown, M. J., Sánchez-Caja, A., Adalid, J.G., Black, S., Pérez Sobrino. M., Duerr, P., Schroeder, S., Saisto, I., (2014), "Improving Propeller Efficiency Through Tip Loading," Proc. of the 30th Symposium on Naval Hydrodynamics, Hobart, Australia.

He, L. (2010) "Numerical Simulation of Unsteady Rotor/Stator Interaction and Application to Propeller/Rudder Combination" PHD dissertation, CAEE, UT Austin.

Hsiao, C.-T., & Chahine, G. L. (2004), "Numerical Study of Cavitation Inception due to Vortex/Vortex Interaction in

a Ducted Propulsor," Proc. of the 25th Symposium on Naval Hydrodynamics, St. John's, Newfoundland and Labrador, CA.

Hunt, J.C.R., Wray, A. & Moin P., (1988), "Eddies, stream and convergence zones in turbulent flows," Center for Turbulence Research Report CTR-S88, Stanford University, Stanford, CA, United States.

Kim, S.-E., Schroeder, S. D., & Jasak, H., "A Multi-Phase CFD Framework for Predicting Performance of Marine Propulsors," (2010) Proc. Of the Thirteenth International Symposium on Transport Phenomena and Dynamics of Rotating Machinery, Moana Surf, USA.

Michael, T., Jessup, S., & Wilson, M. (2000), "Quiet propeller design for a fisheries research vessel," Proc. of the 2000 SNAME Propellers and Shafting Symposium, Virginia Beach, VA.

Nicoud, F. & Ducros, F., (1999), "Subgrid-scale stress modelling based on the square of the velocity gradient tensor." Flow, Turbulence and Combustion, 62, 183-200.

Posa, A., Lippolis, A., Verzicco, R. & Balaras, E. (2011). Large-eddy simulations in mixed-flow pumps using an immersed boundary method. *Computers and Fluids, 47*(1), 33-43.

Posa, A., Lippolis, A., & Balaras, E. (2015). Large-eddy simulations of a mixed-flow pump at off-design conditions. ASME J. Fluids Eng. *In Press.*

Schroeder, S. D., (2014), High Fidelity Numerical Investigation of Rotor Wake Dynamics in the Near Field, PH.D dissertation, George Washington University.

Schroeder, S., Posa, A. & Balaras, E., (2014), "Tip Vortex Evolution of a Marine Propeller Including the Effects of an Upstream Appendage," Proc. of the 30th Symposium on Naval Hydrodynamics, Hobart, Australia.

Weickert, M., Teike, G., Schmidt, O. & Sommerfeld, M. (2010), "Investigation of the LES WALE turbulence model within the lattice Boltzmann framework." Computers and Mathematics with Applications, Vol. 59, No. 7, 2200-2214.

Yang, J. (2005), An Embedded-boundary Formulation for Large-eddy Simulation of Turbulent Flows Interacting with Moving Bodies, PH.D dissertation, University of Maryland.

DISCUSSION

Question from Prof. Yin Lu Young

1) Did the LES model include a cavitation model?
2) Did you build the mesh according to the as-built geometry at the tip; how sensitive was it to the detail geometry at the end plate?
3) Did you measure the detailed differences in the geometry of the different blades to see what is responsible for the difference in tip vortex pattern, where cavitation forms much more downstream and appears more as one vortex than the two co-rotating vortex pattern observed on the other blades?

Author's Closure

Thank you for your questions. The LES performed here was single-phase and did not include a cavitation model. Therefore the results presented are more accurate for sub-cavitating speeds. The large-scale features of the tip vortices (i.e. pitch angle, contraction ratio) are not expected to change very much due to the presence of vapor in the vortex core. This expectation is supported by the good correlation between the present LES results and the water tunnel experiments.

The propeller blade geometry used for the computations were the designed surfaces provided to the model manufacturer. The model was inspected using a digital coordinate measuring machine (CMM) and the model was deemed suitable for testing using the tolerances recommended by the International Towing Tank Conference (ITTC 7.5-01-01-01 and 7.5-01-02-02). It would be an interesting study to examine the differences in LES results between the designed surfaces and the slightly different "as-built" surfaces. However, developing new blade surfaces using the results from the CMM is a process that includes its own difficulties and uncertainties and was not within the scope of this project.

However, it is not certain that these inconsistencies are based solely on differences between the blade surfaces of the model. Tip vortex cavitation exists in a turbulent shear flow and therefore will be inherently unsteady. Furthermore, the cavitation itself is influenced not only by the pressure in the tip vortex, but also by the air content in the tunnel and the presence of nuclei around which the cavitation bubbles form. Both of these additional parameters are not necessarily uniform throughout the fluid. High-speed video can enhance our understanding of flow structures by revealing their movements but it does not necessarily provide the average flow structure or cavitation shapes.

Question from Eckhard Praefke

While I am impressed by the LES results, my question refers rather to a basic issue: why has the design KT value been chosen as high as 0.4? Was this choice a result of efficiency optimization of was a result of cavitation/noise considerations?

Author's Closure

Thank you for your compliment and your question. Our parametric studies discussed in Brown et al. (2014) indicate that propellers designed with tip-loading and end-plates have a greater efficiency advantage over conventional designs in cases of relatively high thrust-loading coefficient (CT) and low advance ratio (J). Therefore, to study and

demonstrate this technology we chose a notional case where the prime mover, along with other practical requirements, specified a CT of 1.27, a diameter of 6.5 meters and rotational speed of 80 RPM. When combined with the expected full power ship speed and wake fraction, this works out to a required KT of 0.42.

Question from Dr. Tom van Terwisga

Did you consider a more gradual distribution of tip rake (like as done in a Kappel propeller) to avoid the small radii of curvature and make them thereby less sensitive to cavitation inception?

Author's Closure

Thank you for your question. In our parametric studies considering tip-loaded propellers (discussed in Brown et al. 2014) we found that there was a small efficiency benefit to having a more localized tip-rake distribution. You are correct, however, that areas with small curvature radii in the blade surface are prone to cavitation. Therefore, during the design process the minimum radius of curvature was implemented that maintained the cavitation inception requirement.